





Optimized coagulation of humic acid and mineral turbidity at alkaline pH using high basicity PACl

Kanika Saxena  and Urmila Brighu 

ABSTRACT

In this study, the simultaneous removal of inorganic turbidity and organics was investigated at alkaline pH to avert the need for pH adjustment and overdosing. The aim was to compare the doses for conventional and enhanced coagulation and, consequently, arrive at optimized coagulation where both had synergistic maximum removal. High basicity PACl was used to coagulate simulated waters prepared by humic acid (HA) and kaolin. The removal of turbidity, total organic carbon (TOC), dissolved organic carbon (DOC) and UV₂₅₄ was evaluated. The impact of varying input concentrations of HA and turbidity on doses was studied. The enhanced coagulation doses were higher than conventional ones. However, with an increase in input TOC, the difference between enhanced and conventional doses narrowed. The doses for optimized coagulation ranged from 2 to 9 mg Al/L. At optimized coagulation, the removal of TOC, DOC and UV₂₅₄ varied from 30–85%, 30–89% and 73–91% respectively. Fourier transform infrared (FTIR) spectroscopy revealed the presence of Si-O-C bond. The interactions of unsaturated bonds of hydrophobic organics to inorganic clay were possibly favoured over hydrophilics. HA agglomeration reduced coagulant consumption as the input TOC increased. It was concluded that instead of a stoichiometric approach, a modified dosing approach can be applied for limiting underdosing and overdosing while ensuring maximum removal of impurities.

Key words | coagulation dosing, enhanced coagulation, humic acid and kaolin interactions, NOM removal, optimized coagulation, polyaluminium chloride

Kanika Saxena  (corresponding author)
Urmila Brighu 
Malaviya National Institute of Technology Jaipur,
Jaipur,
India
E-mail: 2016rce9025@mnit.ac.in

HIGHLIGHTS

- Simultaneous optimized removal of inorganic turbidity and dissolved and particulate organic matter.
- Doses for enhanced coagulation were higher than that for conventional coagulation.
- Modified dosing approach avoids underdosing and overdosing.
- With an increase in input TOC and turbidity, the difference between the dose for enhanced and conventional coagulation narrowed.
- Favoured interaction of hydrophobic organics over hydrophilic organics revealed by FTIR spectroscopy.

INTRODUCTION

The process of coagulation-flocculation is vital, not only for the removal of suspended solids, it also enhances the efficiency of subsequent treatment units such as rapid sand filters, membrane filters, dissolved air flotation, adsorption,

ion-exchange, advanced oxidation processes, etc (Carroll *et al.* 2000; Jiao *et al.* 2017; Sillanpää *et al.* 2018). To keep any technology intact, it is important to optimize and modify it according to the changes in pertinent domain. In

the case of coagulation-flocculation for drinking water, the source water quality is known to alter and influence the efficiency of the process and consequently the overall efficiency of a water treatment plant. Lately, the intrusion of NOM (natural organic matter) due to climate change and man-made activities has increased in the source waters. The potential of NOM to form DBPs (disinfection by-products) is well known (Gheraout 2014; Michael-kordatou *et al.* 2015). Moreover, the fluctuating nature of organics both in quantity and quality due to seasonal changes has affected the efficiency of various water treatment units, particularly clariflocculators which have been optimized traditionally for turbidity removal. This variation in the quality and quantity of NOM has called for the optimization of coagulation-flocculation not only for turbidity removal (conventional coagulation) but also for efficient NOM removal (enhanced coagulation).

Generally, the normal pH range of source waters is near neutral or alkaline and it is known that the optimum pH for NOM removal is on the slightly acidic range (Volk *et al.* 2000). The shifting of pH to the acidic range for optimum NOM removal and further readjustment of pH require the addition of extra chemicals, thus increasing the chemical cost. Therefore, optimizing the removal of NOM along with turbidity using pre-hydrolysed coagulants at near-neutral or alkaline pH is rather a convenient approach. Generally, it is thought to increase the coagulant dose for efficient NOM removal, which may be uncalculated and excessive. On the one hand, the stringent regulations on the acceptable residual coagulant level, especially the residual aluminium in the distributed water, require control on overdosing. On the other hand, under-dosing the coagulant may lead to low treatment efficiency and insufficient removal of impurities, leading to a failure to meet the water quality standards. Therefore, an evaluation of the optimum coagulant dose is important to satisfy these two criteria (Bouyer *et al.* 2001). It becomes important to optimize the removal of impurities simultaneously and evaluate the differences in the dose for conventional and enhanced coagulation to avoid overdosing and underdosing.

Recent studies in the field of coagulation have been more concentrated on the effect of characteristics of NOM (hydrophobic/hydrophilic ratio) on the coagulation process, optimization of pH for NOM removal, development of

novel coagulants, comparison of coagulants, electrocoagulation, hybrid coagulation processes, etc. (Alimohammadi *et al.* 2017; Choudhary & Mathur 2017a, 2017b; Özyurt Camcıoğlu & Hapoglu 2017; Arhin *et al.* 2018). For instance, Liu *et al.* compared two coagulants, AlCl_3 and PACl for the removal of dissolved organic carbon (DOC) and turbidity (Liu *et al.* 2019). Lin *et al.* worked on a dual dosing approach by using FeCl_3 and PACl (Lin & Ika 2019). Yan *et al.* worked for the development of a composite coagulant (HPAC) (Yan *et al.* 2006). Davis and Edwards studied the effect of calcium in coagulation of NOM by using FeCl_3 as a coagulant (Davis & Edwards 2017). Chow *et al.* reported the effect of characteristics of NOM on coagulation (Chow *et al.* 2009). An understanding of dosing requirements for simultaneous removal of NOM and turbidity at alkaline pH and a comprehensive comparison of conventional and enhanced coagulation still needs to be done. For this, it becomes important to study the interactions that might take place between NOM and inorganic turbidity. The interaction of HA with various metal cations has been reported recently to ascertain its capacity for metal sequestration and transport (Tan *et al.* 2019). However, the interaction of HA with inorganic turbidity in context to coagulation stills needs to be explored. The literature still lacks an empirical approach on the effect of fluctuations in NOM and turbidity on the dose of coagulant.

The aim of this study is to compare conventional (turbidity removal) and enhanced (NOM removal) coagulation and consequently arrive at optimized coagulation. The target of optimized coagulation is to maximize the simultaneous removal of inorganic turbidity and total organic carbon (TOC) and to optimize the use of coagulant in order to avoid underdosing or overdosing. The optimized doses obtained from this work are to be scaled up to pilot scale reactors of sludge blanket clarifier and conventional clarifier, for a comprehensive study elaborating the comparison of these two reactors for NOM removal. However, the scope of this research paper is limited to the bench scale studies.

The prime objectives of this work are as follows:

- To compare conventional and enhanced coagulation while evaluating the effect of fluctuating organics and turbidity on the requirement of PACl dose at alkaline pH.
- To quantify the removal efficiencies and residual concentration of inorganic turbidity, TOC, DOC and UV_{254} at

various coagulant doses to evaluate the process efficiency.

- To elaborate the interactions of HA and inorganic turbidity by using Fourier transform infrared (FTIR) spectroscopy and to understand the role of particle concentration in the modification of surface groups of humic acid to interpret the synergies that may affect the mechanisms of coagulation.

MATERIALS AND METHODS

Sample water preparation

To simulate organics, humic acid stock solution was prepared by dissolving powdered humic acid in deionized water. The TOC and DOC of the resulting solution was 736.9 mg/L and 651.1 mg/L, respectively. To simulate turbidity, a stock kaolin suspension in tap water was prepared using powdered kaolin. About 20 g kaolin in 1 L of tap water resulted in turbidity of 70 NTU. After diluting and mixing the stock solutions/suspensions, different suspensions were prepared by varying TOC from 0 to 10 mg/L (0, 2, 4, 6, 8, 10 mg/L) and turbidity from 0 to 20 NTU (0, 5, 10, 15, 20 NTU), to simulate the surface water conditions in the area of this study. The sample water preparation has been elaborately explained in our previous work (Saxena Brighu & Choudhary 2019).

Coagulant

High basicity PACl (Liquid grade, Aditya Birla Chemicals) was used to coagulate the sample waters. The basicity value of the coagulant ranged from 50 to 70%. The content of Al_2O_3 was 10.2–10.5% (weight/weight). The coagulant dose throughout this work is expressed as mg Al/L. 1 mg Al/L corresponds to 18.14 mg of PACl solution having a volume of 15.12 μL . Some pre-feasibility experiments were also performed using PACl on actual surface water samples. The residual aluminium varied from 0.009 to 0.021 mg/L, which was less than the acceptable limit of 0.03 mg/L (Indian Standard Drinking Water – Specification (Second Revision) 2012).

Bench scale setup

A six-paddle jar test apparatus was used to coagulate the synthetically prepared sample waters. Each test water was coagulated by varying the doses of PACl to ascertain the dose of optimal removal of both turbidity and TOC. Rapid mixing was allowed for 2 minutes at 100–150 rpm (hydraulic gradient $G = 330\text{--}610 \text{ s}^{-1}$) and slow mixing was allowed for 20 minutes at 30 rpm (hydraulic gradient $G = 30 \text{ s}^{-1}$) followed by a settling period of 30 minutes (Hendricks 2012). Then the supernatant was pipetted out for further analysis.

Analysis of interaction between humic acid and kaolin in suspension

FTIR spectroscopy (Spectrophotometer- Perkin Elmer Spectrum version 10.4.00) was used to characterize solutions of kaolin and humic acid for the presence of various chemical bonds. The infrared spectrum range was $4,000\text{--}400 \text{ cm}^{-1}$. The input humic acid and kaolin concentration was varied to prepare suspensions having low and high TOC; that is, 2 and 10 mg/L respectively; and input turbidity of 5 and 20 NTU. These values of TOC and turbidity were chosen in accordance with the present surface water conditions in the area of this study; that is, Rajasthan, India. This study is to be further scaled up for the pilot studies for the Bisalpur Water treatment plant in Rajasthan, India (Saxena Brighu & Choudhary 2020). Also, the literature was reviewed extensively to decide the turbidity and TOC values (Saxena Brighu & Choudhary 2018). These impurities were allowed to undergo slow mixing (at 30 rpm for 20 minutes) as in a jar test experiment, so that they interact with each other without the addition of coagulant. This experiment was done to elaborately understand the role of particle concentration and interactions that may affect the process of coagulation, since the dose for NOM removal cannot be adjusted stoichiometrically, as the interactions between hydrophobic organics and inorganic clay minerals result in agglomeration and thus reduce the coagulant demand at high input TOC.

Analytical methods

The treated supernatant, as well as the untreated sample waters, were analyzed for turbidity, TOC, DOC, UV_{254} ,

zeta potential, pH and alkalinity. The equipment and methods used are mentioned in our previous work (Saxena Brighu & Choudhary 2019). The analysis of residual aluminium in this study was performed by Eriochrome cynaine R method 3500-B (APHA 2012). All the experimental analyses were performed in triplicates.

RESULTS AND DISCUSSION

Characterisation of sample waters

The pH of sample waters was on the alkaline side. The alkalinity was high, ranging from 180 to 205 mg/L as CaCO_3 . The pH ranged from 8.14 to 8.45. The SUVA values were >4 for all the sample waters. The zeta potential of the suspensions was on the negative side and ranged from -7.63 to -18.0 mV. The solutions having only TOC (no turbidity) of 2, 4, 6, 8, and 10 mg/L showed a zeta potential of -15.8 , -15.7 , -14.7 , -14.0 and -16.3 mV respectively. The suspensions having only turbidity (no TOC) of 5, 10, 15 and 20 NTU turbidity showed a zeta potential of -7.63 , -16.1 , -16.8 and -18.0 mV respectively. It is apparent that TOC as low as 2 mg/L showed comparable zeta potential to high TOC of 4–10 mg/L and high turbidity of 10–20 NTU. Therefore, the solutions having low TOC were also quite stable because of the high negative charge.

Interaction of humic acid and kaolin in suspension

FTIR spectroscopy is a powerful tool for identifying the presence of functionalities such as unsaturation (double or triple bond), aromaticity, linear chains or branched chains and functional groups. The vibrational or the infrared spectrum of any molecule is its fundamental and unique property formed as a result of absorption of electromagnetic radiation at the frequency that correlates with the vibration of chemical bonds in a molecule (Coates 2000; Stuart 2005).

The FTIR spectrum of humic acid solution is shown in Figure 1 (additional details of the functional groups corresponding to each peak are shown in Appendix A). The peak at $3,383\text{ cm}^{-1}$ can be attributed to the normal polymeric OH stretch due to alcohols. The peak at $1,960\text{ cm}^{-1}$ can be attributed to the substitution pattern of a benzene ring, which appears in the band of $2,000\text{--}1,700\text{ cm}^{-1}$ showing a series of weak combination and overtone bands. The peak at $1,579\text{ cm}^{-1}$ can be attributed to skeletal vibrations, representing aromatic $\text{C}=\text{C}$ stretching, which absorbs in the $1,650\text{--}1,430\text{ cm}^{-1}$ range. The peak at $1,029\text{ cm}^{-1}$ could be due to C-H bending bands in a benzene ring which appears in the $1,275\text{--}1,000\text{ cm}^{-1}$ range. Also, C-O stretching in alcohols and phenols produces a strong band in the $1,300\text{--}1,000\text{ cm}^{-1}$ region. The peak at 917 cm^{-1} could be due to aromatic P-O stretching, which appears in the $1,050\text{--}870\text{ cm}^{-1}$ range. The peak at $2,928\text{ cm}^{-1}$ could be

Spectrum

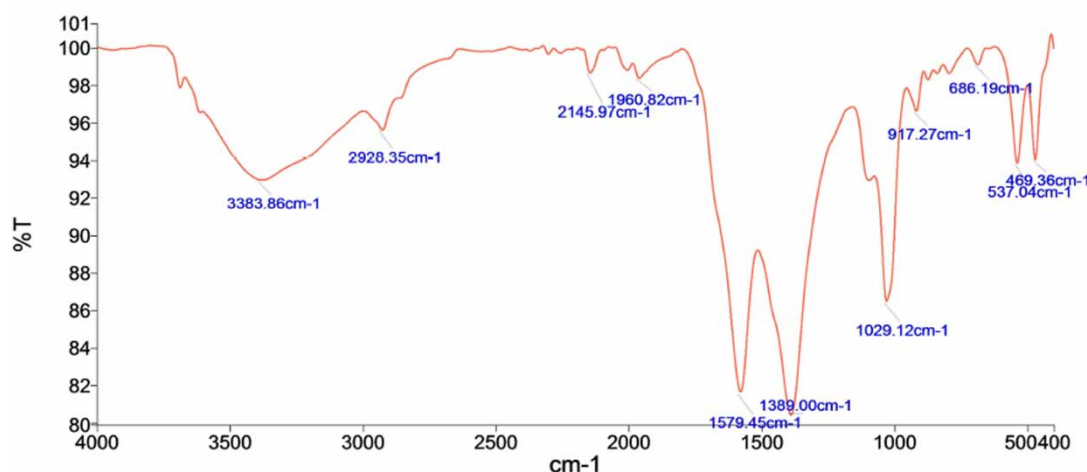


Figure 1 | FTIR spectrum of humic acid stock solution (TOC = 736.9 mg/L).

due to carboxylic acids as they show a strong broad O-H stretching band in the $3,300\text{--}2,500\text{ cm}^{-1}$ range. Also, C-H stretching bands in aliphatic hydrocarbons appear in the $3,000\text{--}2,800\text{ cm}^{-1}$ range. The peak at $2,928\text{ cm}^{-1}$ can also be attributed to methylene groups as they show asymmetric stretching near $2,930\text{ cm}^{-1}$. The peak at $1,389\text{ cm}^{-1}$ can be attributed to trimethyl or tertbutyl. The peak at $1,389\text{ cm}^{-1}$ could also be due to the aliphatic NO_2 group. The peak at $2,145\text{ cm}^{-1}$ can be attributed to aliphatic C=C stretching, which appears in the $2,260\text{--}2,100\text{ cm}^{-1}$ range. The peaks at 469 , 537 , and 686 cm^{-1} can be attributed to aliphatic halogen compounds; that is, C-X stretching [X = Cl, Br or I] (Coates 2000). The peak at 686 cm^{-1} could also be due to aliphatic C-H bending appear in the $700\text{--}600\text{ cm}^{-1}$ range (Stuart 2005). This spectrum shows the presence of aliphatic compounds along with aromatic compounds in humic acid.

The FTIR spectrum of kaolin suspension is shown in Figure 2. A broad peak at $3,499\text{ cm}^{-1}$ is seen, which could be due to O-H stretching for clay minerals, which appears in a range of $3,800\text{--}3,400\text{ cm}^{-1}$. The inner hydroxyl groups between the tetrahedral and octahedral sheets result in a band near $3,620\text{ cm}^{-1}$. The other three O-H groups at the octahedral surface form weak hydrogen bonds with the oxygens of the Si-O-Si bonds in the next layer and this results in stretching bands at $3,669$ and $3,653\text{ cm}^{-1}$. However, these distinctive bands cannot be seen here, probably due to overlapping. Generally, the broad band at $3,750\text{--}3,400\text{ cm}^{-1}$ is

attributed to the surface structural hydroxyl groups of the layered aluminosilicates and adsorbed water. A series of bands located at $1,400\text{--}400\text{ cm}^{-1}$ could be attributed to the lattice vibration of clay minerals (Du & Yang 2012). The peak at $1,054\text{ cm}^{-1}$ could be due to Si-O stretching and bending and O-H bending bands in the $1,300\text{--}400\text{ cm}^{-1}$ region. Kaolinite clays mainly have Al(III) in the octahedral position, due to which several well-resolved strong bands in the $1,120\text{--}1,000\text{ cm}^{-1}$ region are observed (Stuart 2005). The peak at $2,143\text{ cm}^{-1}$ could be due to Si-H stretching, which appears in the range of $2,250\text{--}2,100\text{ cm}^{-1}$. The peak at $1,423\text{ cm}^{-1}$ can be attributed to the presence of the carbonate ion, which shows absorbance in the range of $1,490\text{--}1,410\text{ cm}^{-1}$ (Coates 2000; Stuart 2005).

In the mixed HA and kaolin suspensions, the presence of new peaks (Figure 3) shows the possible interactions between the two types of impurities. The peak at $2,928\text{ cm}^{-1}$ in stock HA is not present in the mixed suspensions, indicating the possibility of the reaction of unsaturated C=O of carboxylic acid to Si resulting in the formation of Si-O-C bond. The new peaks at $1,097$, $1,116$, and $1,068\text{ cm}^{-1}$ could be attributed to Si-O-C stretching as the Si-O-C stretching produces a broad band at $1,100\text{--}1,050\text{ cm}^{-1}$. Also, silicon attached to a benzene ring produces two strong bands near $1,430\text{ cm}^{-1}$ and $1,110\text{ cm}^{-1}$. Aromatic organometallic molecules also show a strong band near $1,430\text{ cm}^{-1}$, due to benzene ring

Spectrum

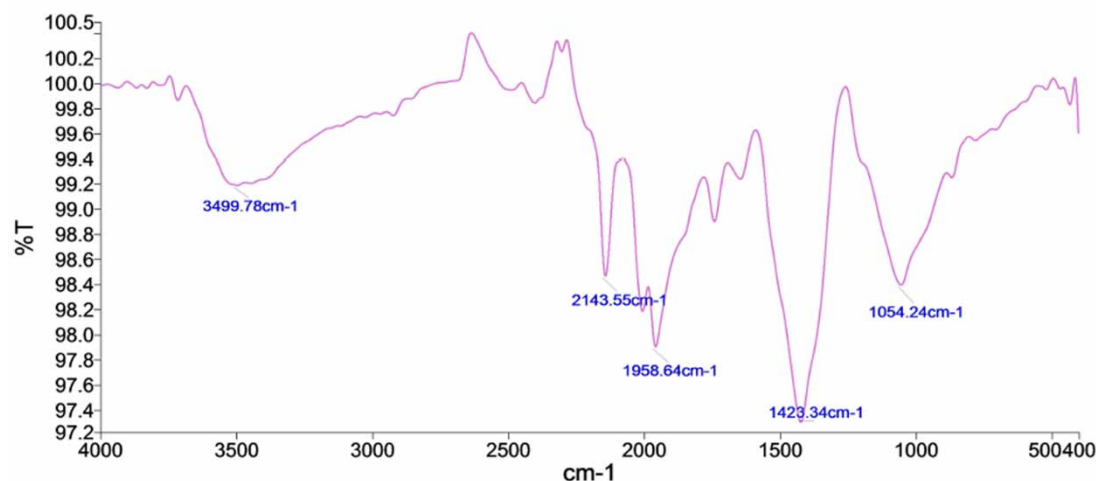


Figure 2 | FTIR spectrum of kaolin stock suspension (Turbidity = 70 NTU).

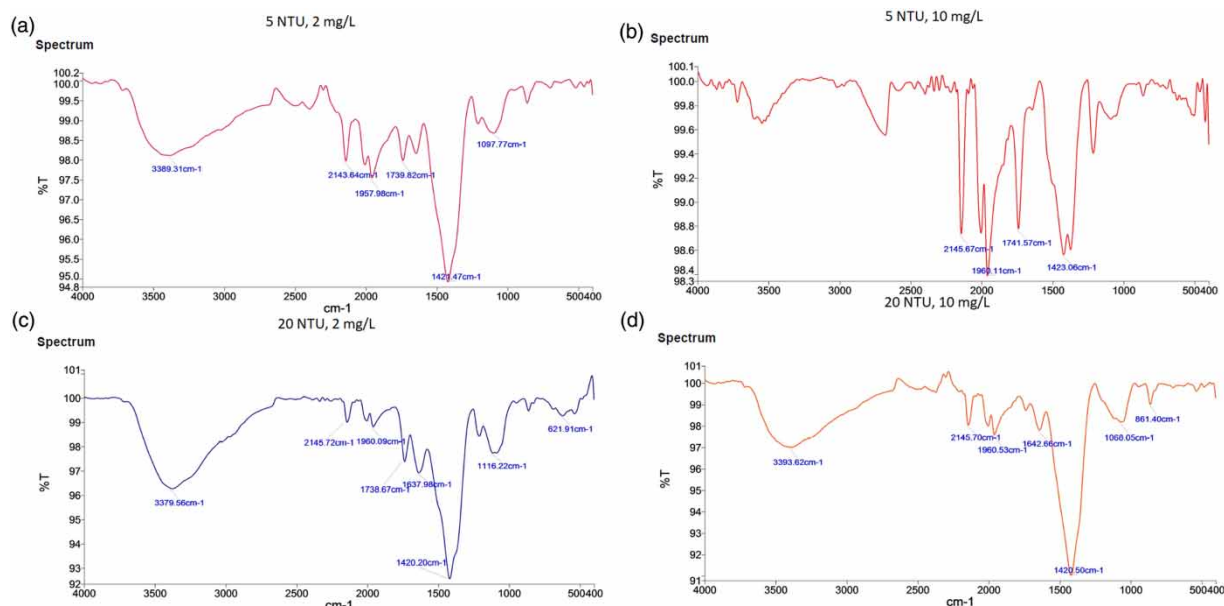


Figure 3 | FTIR spectra of mixed kaolin and humic acid solution.

stretching for metals directly attached to the benzene ring. The presence of new peaks near $1,740\text{ cm}^{-1}$ could also be due to the aliphatic $\text{C}=\text{O}$ stretching. The peak at $1,579\text{ cm}^{-1}$ attributed to aromatic $\text{C}=\text{C}$ has disappeared in mixed suspensions. Also, the presence of new peaks ($1,637$ and $1,642\text{ cm}^{-1}$) in case of high turbidity of 20 NTU could be due to aliphatic $\text{C}=\text{C}$ stretching (Stuart 2005). The peak at $1,389\text{ cm}^{-1}$ of the stock HA, possibly due to attached NO_2 group, also disappears in the mixed suspensions. In case of 20 NTU and 10 mg/L TOC, a new peak at 861 cm^{-1} is seen possibly due to N-O stretching. Also, the bands which were previously present in HA in the range of $800\text{--}400\text{ cm}^{-1}$, possibly due to halogenated compounds (Figure 1), are subdued in the mixed suspensions. The new peaks in the mixed suspensions are more concurrent with the aliphatics than aromatics. It is known that hydrophilic DOM (dissolved organic matter) comprises more aliphatic carbon and aliphatic nitrogenous compounds, whereas hydrophobic DOM comprises more aromatic and phenolic compounds. Also the specific colloidal charge of hydrophobics is higher than hydrophilics (Matilainen *et al.* 2011; Saxena Brighu & Choudhary 2018). This suggests that the interactions of unsaturated bonds of hydrophobics ($\text{C}=\text{O}$ of carboxylic acids, $\text{C}=\text{C}$ of aromatic rings) to

inorganic clay are possibly favoured over hydrophilics due to their higher colloidal charge.

The interactions between these two types of impurities may further be affected by the presence of alkalinity. The presence of high alkalinity, which is generally due to carbonates and bicarbonates of Mg^{+2} and Ca^{+2} , can significantly suppress the solubility of HA by bonding with them and forming macromolecules. The deprotonation increases with pH and metal cations can interact with negative functional groups such as phenolic and carboxylic groups of HA. Ca^{+2} can interact with one or more HA molecules thus reducing their net negative charge and bringing them together to agglomerate. These interactions are pH-dependent; for instance, Ca^{+2} binds with carboxylic groups at lower pH and phenolic groups at higher pH (Kinniburgh *et al.* 1999). The carboxylic group forms a strong association with Mg^{+2} compared to the phenolic group (Ahn Kalinichev & Clark 2008). The greater charge density on Mg^{+2} makes its bonding considerably faster and stronger compared to Ca^{+2} (Adusei-Gyamfi *et al.* 2019). In this study, it is possible that the presence of high alkalinity further promotes the aggregation by attachment of Ca^{+2} with the aromatic phenolic groups and Mg^{+2} with aromatic/aliphatic phenolic and carboxylic groups. This further confirms more possibilities of reaction of aromatic phenolic/carboxylic groups than

the aliphatic ones, as the aliphatics preferably react with Mg^{+2} and aromatics can react with both.

In nutshell, it was observed that interactions of the unsaturated bonds of the functional groups of hydrophobic organic matter to inorganic clay were favoured over hydrophilics, resulting in agglomeration of humic acid without coagulant aid.

Turbidity removal: conventional coagulation

Baseline or conventional coagulation has been applied traditionally in water treatment to decrease turbidity and pathogens (Volk *et al.* 2000). In this study, the optimum

dose for baseline coagulation was defined as the dose required to reduce the residual turbidity below 1 NTU. As the dose of PACl increased, the residual turbidity decreased and further increased in some cases possibly due to restabilization. However, in some cases, the residual turbidity plateaued and showed no further major decrease or increase with increasing doses (Figure 4).

For different input levels of TOC and turbidity, the optimum doses were evaluated (Table 1). For low input turbidity of 5 NTU, there is an increase in the dose as the input TOC increased. A similar trend can be seen for input turbidity of 10 NTU and 15 NTU. This shows

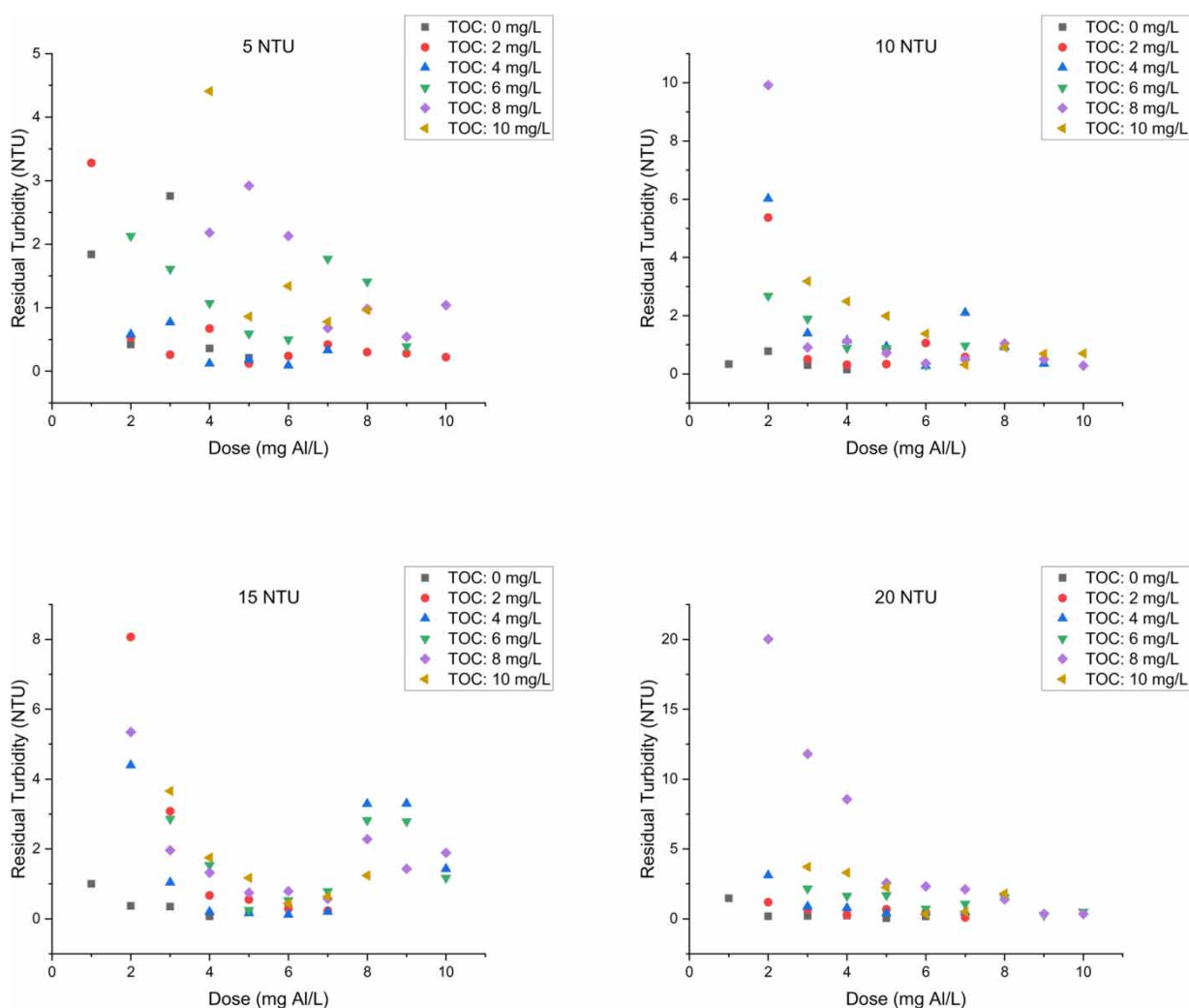


Figure 4 | Residual turbidity values at various doses of PACl.

Table 1 | Optimum doses of PACl for conventional coagulation (mg Al/L)

Input turbidity (NTU)	Input TOC (mg/L)					
	0	2	4	6	8	10
5	2	2	2	5	7	7
10	2	3	5	4	5	7
15	2	4	4	5	5	6
20	2	3	3	6	9	6

that NOM is essentially controlling the dose requirement for input turbidity ≤ 15 NTU. But in the case of 20 NTU, the optimum dose first increased with increasing input TOC and then decreased when the input TOC was very high; that is, 10 mg/L. This could be due to efficient settling of heavier or compact flocs formed due to high collision frequency. The increased particle collision rate due to a large number of particles per unit volume could have possibly resulted in efficient agglomeration or attachment of particles. It has also been reported earlier that the presence of HA leads to better floc formation in kaolin simulated water (Lin *et al.* 2003).

For the variation of optimum doses with constant input TOC and increasing turbidity, the optimum doses for 0 initial TOC remained unchanged with increasing turbidity. For an initial TOC of 2 mg/L, the optimum dose first increased and then again decreased with increasing turbidity. A similar trend was seen for input TOC of 4 mg/L. For input TOC of 6 and 8 mg/L, there was a slight change in the trend. An initial drop in the optimum dose and then an increment was seen as the turbidity increased. For input TOC of 10 mg/L, there was a marginal decrease in the optimum dose with increasing turbidity. It can be concluded that as the particle concentration gradually increased, the optimum dose increased and with a further increase in the particle concentration an improved floc formation essentially led to a decrease in the optimum dose. But again, with a further increase in the particle concentration, the requirement for the dose may increase. Therefore, it can be said that there is a range of particle concentration where there is a reduced requirement of coagulant. However, on either side of this range, there is an increase in the dose requirement.

NOM removal: enhanced coagulation

For optimising the dose for NOM removal, it is important to quantify NOM before and after coagulation-flocculation in terms of TOC, DOC and UV₂₅₄. In this study, the optimum doses for enhanced coagulation were so selected where the residual TOC reduced to a minimum with increasing PACl dose and beyond which even after increasing the dose no further appreciable reduction in TOC was observed. The optimum doses for different input levels of TOC and turbidity are shown in Table 2. For low input TOC of 2 and 4 mg/L, the optimum doses remained almost similar irrespective of increasing turbidity. For input TOC of 6 and 8 mg/L, the optimum doses increased with increasing turbidity. At input TOC of 10 mg/L, the optimum doses first increased and then decreased with increasing turbidity. At the optimum doses, the residual TOC varied from 0.749 to 2.004 mg/L and the mean residual TOC increased as the input TOC increased (Figure 5). The TOC removal percentage varied from 30 to 85% at optimized doses.

The DOC removal was evaluated to assess the removal efficiency of the dissolved portion of NOM. The complete removal of DOC was difficult at alkaline pH. The residual DOC ranged from 0.5 to 1.4 mg/L at optimum doses for TOC removal (Figure 6). The mean residual DOC also increased as the input TOC increased. The percentage DOC removal varied from 30 to 89% at optimum doses. The smaller size fraction or the hydrophilic fraction of DOM could be possibly difficult to remove as the dominant mechanism at alkaline pH is sweep coagulation rather than charge neutralization. The results of this work have been used to elucidate probable mechanisms using an isotherm study in a previous work (Saxena Brighu & Choudhary

Table 2 | Optimum doses of PACl for enhanced coagulation (mg Al/L)

Input turbidity (NTU)	Input TOC (mg/L)				
	2	4	6	8	10
0	5	6	5	5	6
5	5	6	6	7	7
10	5	6	6	7	7
15	4	7	6	7	7
20	5	6	8	8	6

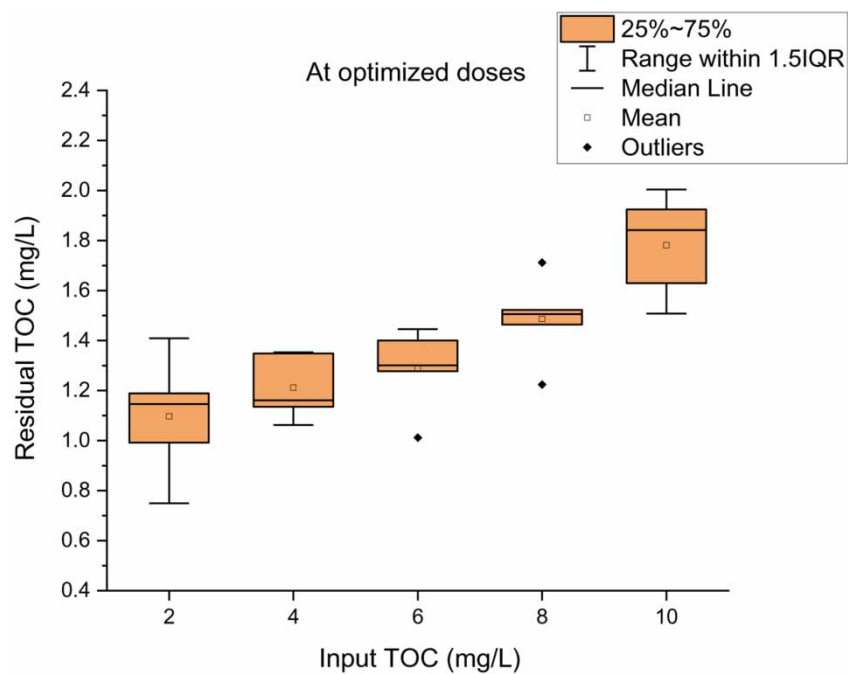


Figure 5 | Residual TOC at optimized doses as mentioned in Table 2 (Optimized doses range - 4–5, 6–7, 5–8, 5–8 and 6–7 mg Al/L for 2, 4, 6, 8 and 10 mg/L of input TOC respectively) (Mean values and standard deviation of residual TOC – 1.10 ± 0.22 , 1.21 ± 0.12 , 1.29 ± 0.15 , 1.49 ± 0.16 and 1.78 ± 0.18 mg/L for 2, 4, 6, 8 and 10 mg/L of TOC respectively).

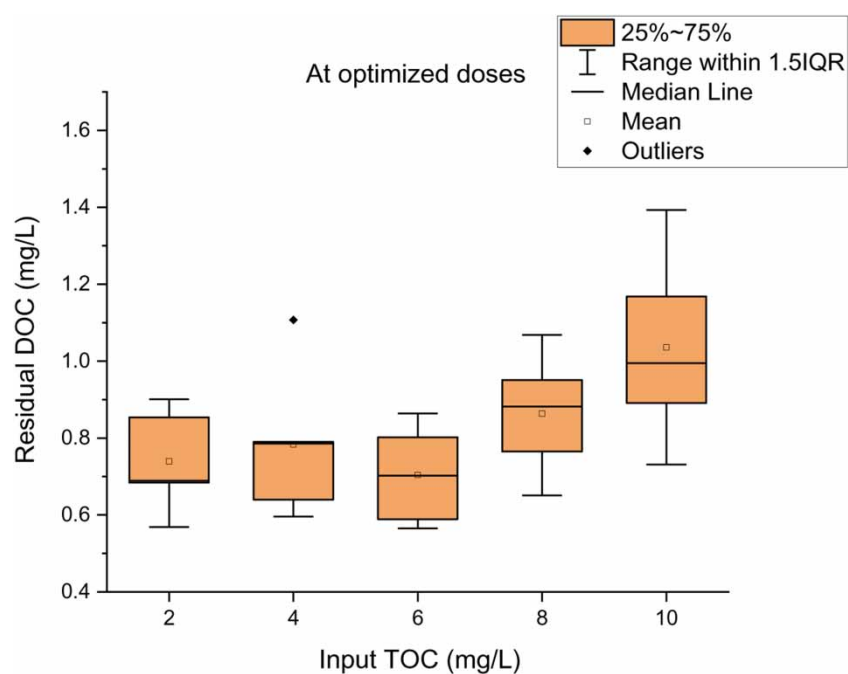


Figure 6 | Residual DOC at optimized doses as mentioned in Table 2 (Optimized doses - 4–5, 6–7, 5–8, 5–8 and 6–7 mg Al/L for 2, 4, 6, 8 and 10 mg/L of input TOC respectively) (Mean values and standard deviation of residual DOC – 0.74 ± 0.12 , 0.78 ± 0.18 , 0.70 ± 0.12 , 0.86 ± 0.14 and 1.04 ± 0.23 mg/L for 2, 4, 6, 8 and 10 mg/L of TOC respectively).

2019). It was found that TOC and turbidity were removed dominantly by entrapment and adsorption on $\text{Al}(\text{OH})_3$ and to a lesser extent by charge neutralization by preformed Al_b species because after the treatment, the zeta potential was still negative (-15.53 to -1.3 mV), pH was above the neutral value (7.65–8.00) and alkalinity was high (140–190 mg/L). Lesser prevalence of charge neutralization could possibly be the reason for the presence of residual DOC in the treated water. It has been previously reported that there is poor removal of the hydrophilic fraction of DOM at the coagulation pH of normal operation (5–7), as the hydrophilic fractions possess a negligible or slightly positive charge (Edzwald 1993; Sharp *et al.* 2006). The hydrophilic portion has hydrated layers surrounding them, which may lead to the confinement of their surface charge within the hydrated layer. The charge of the hydrophilic portion is primarily due to the ionization of functional groups or ligands such as carboxylic, phenolic or other aliphatic and aromatic groups. The precipitation of metal ion-ligand complexes is required for the removal of hydrophilic colloids. These ligands do not have a great affinity for metal ions when compared to OH^- ions. Therefore, for the removal of hydrophilic colloids, acidic pH is preferred when the OH^- ions are lesser and metal ions form complexes with ligands. But when pH is alkaline, a higher coagulant dose may result in the binding of metal ions first to the OH^- ions and then to the functional groups of hydrophilic colloids. As such, a higher dose is required to remove hydrophilic colloids under alkaline conditions and electrostatic interactions play an important role in their removal. On the other hand, the hydrophobic portion of NOM is water repellent and the hydrated layer is thinner than that on the hydrophilic colloids. The adsorption of hydroxyl ions which are present in the coordinated sheath of a coagulant metal ion is understood to be the major removal mechanism. The greater the replacement of water molecules with hydroxyl ions in the coordination sphere of the central metal ion of the coagulant, the greater is the adsorption of coagulant on hydrophobic colloids. Therefore, the removal is enhanced by the presence of neutral species such as $\text{Al}(\text{OH})_3$. In the case of high concentrations of hydrophobic colloids, the double layer compression mechanism may also aid the removal and reduce the coagulant requirement (Bratby 2016). The presence of hydrophobic

portion of DOM can be assessed by measuring the absorbance at 254 nm also known as UV_{254} . The removal of UV_{254} was also measured. The removal percentage plateaued after reaching 70–90% with increasing doses (Figure 7). It has been reported that humic acids and nonpolar groups can easily be adsorbed onto metal hydroxide precipitates (Kastl *et al.* 2004). Therefore, the efficient removal of UV_{254} portion of NOM can be attributed to the removal by $\text{Al}(\text{OH})_3$.

Simultaneous maximised removal of turbidity and TOC: optimized coagulation

The doses for optimized coagulation were selected where the turbidity reduction was <1 NTU and TOC removal was also maximum. The doses for conventional (CC dose), enhanced (EC dose) and optimized coagulation are mentioned in Table 3. The EC doses were observed to be higher than the CC doses for almost all the input levels of TOC and turbidity and for some cases both were equal. Only in one case, the CC dose was higher than the EC dose. Even in the presence of TOC as low as 2 mg/L the doses were greater for enhanced coagulation. The statistical difference between the means of the two sets of doses; that is, CC and EC, were examined by using a paired t test. The p value was <0.05 , which showed that the two set of doses were statistically different. The differences between the EC dose and CC dose were positive for most of the cases. The differences were least (zero in some case) for high input NOM, indicating improved flocculation in the case of input TOC as high as 8–10 mg/L. The increment factor (i.e. the ratio of EC dose/CC dose in column 7) was least when the input TOC was 10 mg/L, which indicates that the differences between EC and CC doses narrowed when TOC was high, again supporting the fact that the increase in input NOM may reduce the coagulant demand. It appears that optimising the process of coagulation for TOC removal rather than turbidity removal is a better outlook at alkaline pH. However, in the case of higher input turbidity (>15 NTU) coupled with higher input TOC (>10 mg/L) one can go for conventional coagulation.

In Figure 8, the Al used per mg of TOC removed is shown. With increasing input TOC, the consumption of coagulant per unit TOC removed has decreased. This

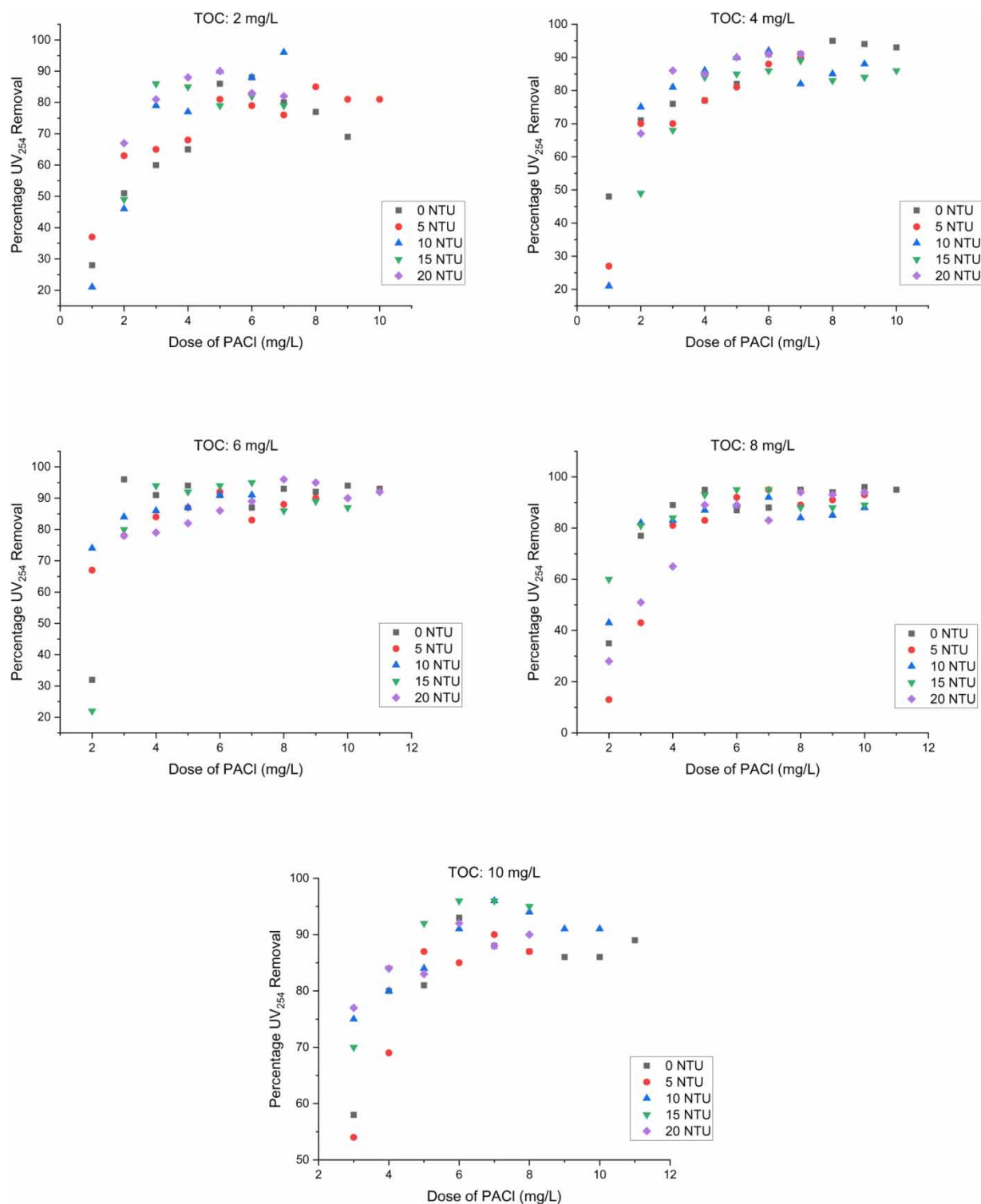


Figure 7 | Percentage UV₂₅₄ removal at various doses of PACI.

Table 3 | Optimum doses for conventional, enhanced and Optimized coagulation

Input turbidity (NTU) (1)	Input TOC (mg/L) (2)	Dose for turbidity removal (Conventional Coagulation) (mg Al/L) (3)	Dose for NOM removal (Enhanced Coagulation) (mg Al/L) (4)	Dose for optimized coagulation (mg Al/L) (5)	Difference of the dose (EC dose – CC dose) (4)–(3) = (6)	Increment factor EC dose/CC dose (7)
0	2	–	5	5	–	
0	4	–	6	6	–	
0	6	–	5	5	–	
0	8	–	5	5	–	
0	10	–	7	7	–	
5	0	2	–	2	–	
5	2	2	5	5	3	2.5
5	4	2	6	6	4	3
5	6	5	6	6	1	1.2
5	8	7	7	7	0	1
5	10	7	7	7	0	1
10	0	2	–	1		
10	2	3	5	5	2	1.7
10	4	5	6	6	1	1.2
10	6	4	6	6	2	1.5
10	8	5	7	7	2	1.4
10	10	7	7	7	0	1
15	0	2	–	2		
15	2	4	4	4	0	1
15	4	4	7	7	3	1.75
15	6	5	6	6	1	1.2
15	8	5	7	7	2	1.4
15	10	6	7	7	1	1.16
20	0	2	–	2		
20	2	3	5	5	2	1.7
20	4	3	6	6	3	2
20	6	6	8	8	2	1.3
20	8	9	8	9	–1	0.89
20	10	6	6	6	0	1

shows that the dose cannot be increased according to the input NOM stoichiometrically. It is a well-established fact that at higher pH values the amorphous precipitate $\text{Al}(\text{OH})_3$ is the dominant species and the removal of NOM is dependent on the adsorption of humic substances on $\text{Al}(\text{OH})_3$ (Kastl *et al.* 2004). Also, the FTIR data revealed the interactions of organic and inorganic impurity resulting in agglomeration of the suspended particles, even in the absence of coagulant. Therefore, the presence of sufficient particle concentration and

$\text{Al}(\text{OH})_3$ possibly resulted in multilayer adsorption of NOM and thus reduced the coagulant demand.

CONCLUSIONS

The major conclusions drawn from this study are as follows:

- The doses for conventional and enhanced coagulation were identified, which ranged from 2 to 9 mg Al/L and

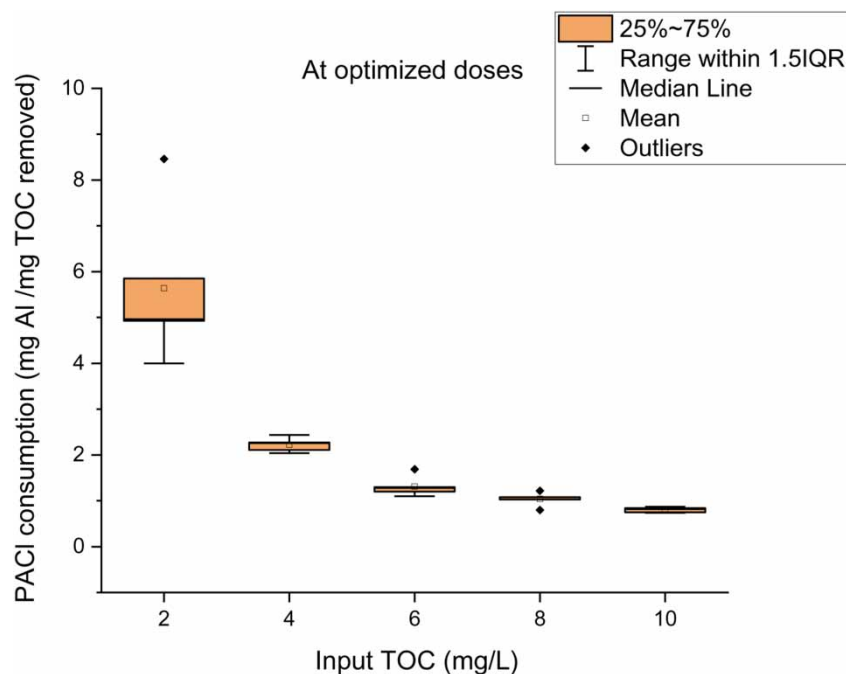


Figure 8 | Consumption of PACl per unit TOC removed at optimized doses (Mean values and standard deviation – 5.64 ± 1.53 , 2.22 ± 0.14 , 1.31 ± 0.20 , 1.04 ± 0.14 , 0.80 ± 0.05 for TOC of 2, 4, 6, 8 and 10 mg/L respectively).

4–7 mg Al/L respectively. The optimized coagulation doses ranged from 2 to 9 mg/L.

- It was found that the doses for enhanced coagulation were higher than the conventional coagulation. The difference between the doses for enhanced and conventional coagulation was however lesser at high input TOC and turbidity. The synergistic removal of TOC and turbidity essentially improved at high input concentration, indicated by a reduction in the optimum dose and coagulant consumption, thus indicating that the doses cannot be increased in the stoichiometric ratios.
- The FTIR spectra revealed the presence of new peaks in the mixed HA and kaolin suspensions due to possible association of the unsaturated bonds of the aromatic hydrophobic organic matter with inorganic clay resulting in the agglomeration of HA without coagulant aid.
- For optimization of the coagulation process, for waters having low input turbidity and NOM ≥ 2 mg/L, optimization for NOM removal may lead to the removal of both the impurities. However, at high input TOC and turbidity, the conventional and enhanced coagulation both might deliver a good performance. Overall, optimizing the process for TOC will essentially result in the removal of turbidity.

- At optimized coagulation, the removal of TOC, DOC and UV₂₅₄ varied from 30–85%, 30–89% and 73–91% respectively. The residual TOC and DOC ranged from 0.7–2 mg/L and 0.5–1.4 mg/L respectively. The efficient removal of UV₂₅₄ indicated that the hydrophobic portion was efficiently removed and the residual was majorly the dissolved hydrophilic portion of NOM.

It can be concluded that by using pre-hydrolyzed coagulants such as PACl, efficient NOM removal can be achieved for raw water with high alkalinity without adjusting the pH to the acidic range. In a nutshell, this study can be used for optimizing or modifying the dosing approaches for full-scale or pilot-scale water treatment plants in order to avoid underdosing (to comply with DBP standards) or overdosing (to comply with residual aluminium standards) and in parallel ensuring maximum removal of organic and inorganic contaminants.

ACKNOWLEDGEMENT

The authors are thankful to the Materials Research Centre MNIT Jaipur for the analysis of zeta potential and FTIR.

DATA AVAILABILITY STATEMENT

All relevant data are included in the paper or its Supplementary Information.

REFERENCES

- Adusei-Gyamfi, J., Ouddane, B., Rietveld, L., Cornard, J.-P. & Criquet, J. 2019 [Natural organic matter-cations complexation and its impact on water treatment: a critical review](#). *Water Research* **160**, 130–147. <https://doi.org/10.1016/j.watres.2019.05.064>.
- Ahn, W. Y., Kalinichev, A. G. & Clark, M. M. 2008 [Effects of background cations on the fouling of polyethersulfone membranes by natural organic matter: experimental and molecular modeling study](#). *Journal of Membrane Science*. <https://doi.org/10.1016/j.memsci.2007.10.023>.
- Alimohammadi, M., Askari, M., Dehghani, M. H., Dalvand, A., Saeedi, R., Yetilmezsoy, K., Heibati, B. & McKay, G. 2017 [Elimination of natural organic matter by electrocoagulation using bipolar and monopolar arrangements of iron and aluminum electrodes](#). *International Journal of Environmental Science and Technology* **14**, 2125–2134. <https://doi.org/10.1007/s13762-017-1402-3>.
- APHA 2012 [Standard Methods for the Examination of Water and Wastewater](#). American Public Health Association (APHA), Washington, DC, USA.
- Arhin, S. G., Banadda, N., Komakech, A. J., Pronk, W. & Marks, S. J. 2018 [Optimization of hybrid coagulation-ultrafiltration process for potable water treatment using response surface methodology](#). *Water Science and Technology: Water Supply* **18** (3), 862–874. <https://doi.org/10.2166/ws.2017.159>.
- Bouyer, D., Line, A., Cockx, A. & Do-Quang, Z. 2001 [Experimental analysis of floc size distribution and hydrodynamics in a jar-test](#). *Chemical Engineering Research and Design* **79** (8), 1017–1024. <https://doi.org/10.1205/02638760152721587>.
- Bratby, J. 2016 [Coagulation and flocculation in water and wastewater treatment](#). *Water* **5** (1), 538. <https://doi.org/10.2166/9781780402321>.
- Carroll, T., King, S., Gray, S. R., Bolto, B. A. & Booker, N. A. 2000 [The fouling of microfiltration membranes by NOM after coagulation treatment](#). *Water Research* **34** (11), 2861–2868. [https://doi.org/10.1016/S0043-1354\(00\)00051-8](https://doi.org/10.1016/S0043-1354(00)00051-8).
- Choudhary, A. & Mathur, S. 2017a [Performance evaluation of 3D rotating anode in electro coagulation reactor: part I: effect of impeller](#). *Journal of Water Process Engineering* **19**, 322–330. <https://doi.org/10.1016/j.jwpe.2017.08.020>.
- Choudhary, A. & Mathur, S. 2017b [Performance evaluation of 3D rotating anode in electro coagulation reactor: part II: effect of rotation](#). *Journal of Water Process Engineering* **19**, 352–362. <https://doi.org/10.1016/j.jwpe.2017.08.019>.
- Chow, C. W. K., van Leeuwen, J. A., Fabris, R. & Drikas, M. 2009 [Optimised coagulation using aluminium sulfate for the removal of dissolved organic carbon](#). *Desalination* **245** (1–3), 120–134. <https://doi.org/10.1016/j.desal.2008.06.014>.
- Coates, J. 2000 [Interpretation of Infrared Spectra, A Practical Approach](#). pp. 10815–10837.
- Davis, C. C. & Edwards, M. 2017 [Role of calcium in the coagulation of NOM with ferric chloride](#). *Environmental Science and Technology* **51** (20), 11652–11659. <https://doi.org/10.1021/acs.est.7b02038>.
- Du, C. & Yang, H. 2012 [Investigation of the physicochemical aspects from natural kaolin to Al-MCM-41 mesoporous materials](#). *Journal of Colloid and Interface Science* **369** (1), 216–222. <https://doi.org/10.1016/j.jcis.2011.12.041>.
- Edzwald, J. K. 1993 [Coagulation in drinking water treatment: particles, organics and coagulants](#). *Water Science and Technology* **27**, 21–35. <https://doi.org/10.1016/0273-1223/93>.
- Gheraout, D. 2014 [The hydrophilic/Hydrophobic ratio vs. dissolved organics removal by coagulation – a review](#). *Journal of King Saud University – Science* **26** (3), 169–180. <https://doi.org/10.1016/j.jksus.2013.09.005>.
- Hendricks, D. 2012 [Water Treatment Unit Processes](#). *Water Treatment Unit Processes*. <https://doi.org/10.1142/p063>.
- Indian Standard, Drinking Water – Specification (Second Revision) 2012.
- Jiao, R., Fabris, R., Chow, C. W. K., Drikas, M., van Leeuwen, J., Wang, D. & Xu, Z. 2017 [Influence of coagulation mechanisms and floc formation on filterability](#). *Journal of Environmental Sciences (China)* **57**, 338–345. <https://doi.org/10.1016/j.jes.2017.01.006>.
- Kastl, G., Sathasivan, A., Fisher, I. & Van Leeuwen, J. 2004 [Modeling DOC removal by enhanced coagulation](#). *Journal of American Water Works Association* **96** (2), 79–89.
- Kinniburgh, D. G., Van Riemsdijk, W. H., Koopal, L. K., Borkovec, M., Benedetti, M. F. & Avena, M. J. 1999 [Ion binding to natural organic matter: competition, heterogeneity, stoichiometry and thermodynamic consistency](#). *Colloids and Surfaces A: Physicochemical and Engineering Aspects* **151**, 147–166. [https://doi.org/10.1016/S0927-7757\(98\)00637-2](https://doi.org/10.1016/S0927-7757(98)00637-2).
- Lin, J.-L. & Ika, A. R. 2019 [Enhanced coagulation of low turbid water for drinking water treatment: dosing approach on floc formation and residuals minimization](#). *Environmental Engineering Science* **36** (6), 1–7. <https://doi.org/10.1089/ees.2018.0430>.
- Lin, W. W., Sung, S. S., Lee, D. J., Chen, Y. P., Chen, D. S. & Lee, S. F. 2003 [Coagulation of humic-Kaolin-PACl aggregates](#). *Water Science and Technology* **47** (1), 145–152.
- Liu, R., Guo, T., Ma, M., Yan, M., Qi, J., Hu, C., Liu, G., Liu, H., Qu, J. & van der Meer, W. 2019 [Preferential binding between intracellular organic matters and Al 13 polymer to enhance coagulation performance](#). *Journal of Environmental Sciences (China)* **76**, 1–11. <https://doi.org/10.1016/j.jes.2018.05.011>.

- Matilainen, A., Gjessing, E. T., Lahtinen, T., Hed, L., Bhatnagar, A. & Sillanpää, M. 2011 [An overview of the methods used in the characterisation of natural organic matter \(NOM\) in relation to drinking water treatment](#). *Chemosphere* **83** (11), 1431–1442. <https://doi.org/10.1016/j.chemosphere.2011.01.018>.
- Michael-kordatou, I., Michael, C., Duan, X. & He, X. 2015 [Direct dissolved effluent organic matter: characteristics and potential implications in wastewater treatment and reuse applications](#). *Science* **77**, 213–248. <https://doi.org/10.1016/j.watres.2015.03.011>.
- Özyurt, B., Camcioğlu, Ş. & Hapoglu, H. 2017 [A consecutive electrocoagulation and electro-oxidation treatment for pulp and paper mill wastewater](#). *Desalination and Water Treatment* **93**, 214–228. <https://doi.org/10.5004/dwt.2017.21257>.
- Saxena, K., Brighu, U. & Choudhary, A. 2018 [Parameters affecting enhanced coagulation: a review](#). *Environmental Technology Reviews* **7** (1), 156–176. <https://doi.org/10.1080/21622515.2018.1478456>.
- Saxena, K., Brighu, U. & Choudhary, A. 2019 [Coagulation of humic acid and kaolin at alkaline pH: complex mechanisms and effect of fluctuating organics and turbidity](#). *Journal of Water Process Engineering* **31** (June), 100875. <https://doi.org/10.1016/j.jwpe.2019.100875>.
- Saxena, K., Brighu, U. & Choudhary, A. 2020 [Pilot-scale coagulation of organic and inorganic impurities : mechanisms, role of particle concentration and scale effects](#). *Journal of Environmental Chemical Engineering* **8** (4), 103990. <https://doi.org/10.1016/j.jece.2020.103990>.
- Sharp, E. L., Jarvis, P., Parsons, S. A. & Jefferson, B. 2006 [Impact of fractional character on the coagulation of NOM](#). *Colloids and Surfaces A: Physicochemical and Engineering Aspects* **286** (1–3), 104–111. <https://doi.org/10.1016/j.colsurfa.2006.03.009>.
- Sillanpää, M., Ncibi, M. C., Matilainen, A. & Vepsäläinen, M. 2018 [Removal of natural organic matter in drinking water treatment by coagulation: a comprehensive review](#). *Chemosphere* **190**, 54–71. <https://doi.org/10.1016/j.chemosphere.2017.09.113>.
- Stuart, B. H. 2005 *Infrared Spectroscopy: Fundamentals and Applications*. Wiley, Hoboken, NJ. <https://doi.org/10.1002/0470011149>.
- Tan, L., Yu, Z., Tan, X., Fang, M., Wang, X., Wang, J., Xing, J., Ai, Y. & Wang, X. 2019 [Systematic studies on the binding of metal ions in aggregates of humic acid: aggregation kinetics, spectroscopic analyses and MD simulations](#). *Environmental Pollution* **246**, 999–1007. <https://doi.org/10.1016/j.envpol.2019.01.007>.
- Volk, C., Bell, K., Ibrahim, E., Verges, D., Amy, G. & Lechevallier, M. 2000 [Impact of enhanced and optimized coagulation on removal of organic matter and its biodegradable fraction in drinking water](#). *Water Research* **34** (12), 3247–3257. [https://doi.org/10.1016/S0043-1354\(00\)00033-6](https://doi.org/10.1016/S0043-1354(00)00033-6).
- Yan, M., Wang, D., You, S., Qu, J. & Tang, H. 2006 [Enhanced coagulation in a typical north-China water treatment plant](#). *Water Research* **40** (19), 3621–3627. <https://doi.org/10.1016/j.watres.2006.05.044>.

First received 20 November 2019; accepted in revised form 17 June 2020. Available online 30 June 2020